

Oxime Functionalization Strategy for Iodinated Poly(ϵ -caprolactone) X-ray Opaque Materials

Samantha E. Nicolau,¹ Lundy L. Davis,¹ Caroline C. Duncan,¹ Timothy R. Olsen,² Frank Alexis,^{2,3} Daniel C. Whitehead,⁴ Brooke A. Van Horn¹

¹Department of Chemistry and Biochemistry, College of Charleston, 66 George St., Charleston, South Carolina 29424

²Department of Bioengineering, Clemson University, 203 Rhodes Research Center Annex, Clemson, South Carolina 29634

³Institute of Biological Interfaces of Engineering, Department of Bioengineering, Clemson University, Clemson, South Carolina 29634-0905

⁴Department of Chemistry, Clemson University, 467 Hunter Laboratories, Clemson, South Carolina 29634

Correspondence to: B. A. Van Horn (E-mail: vanhornba@cofc.edu)

Received 16 March 2015; accepted 13 May 2015; published online 16 June 2015

DOI: 10.1002/pola.27706

ABSTRACT: Since two of the most common technologies for imaging the human body are X-ray radiography and computed tomography (CT), researchers are focused on developing biodegradable and biocompatible polymeric molecules as an alternative to the traditional small molecule contrast agents. This report highlights the synthesis of novel biodegradable iodinated poly(ϵ -caprolactone) copolymers by oxime "Click" ligation reactions. A series of ketone-bearing materials are built by tin (II)-mediated ring-opening polymerization followed by a postpolymerization deprotection step. The intended X-ray opacity is imparted through acid-catalyzed oxime postpolymerization modification of the resultant polymers with an iodinated

hydroxylamine. All small molecules and polymeric materials are characterized using proton nuclear magnetic resonance (NMR) for purity, functional group stoichiometry, and number-averaged molecular weight calculations. Additionally, the polymers are evaluated with gel permeation chromatography (GPC) to determine polymer sample polydispersity and general molecular weight distribution shapes and by differential scanning calorimetry (DSC) and thermogravimetric analysis (TGA) for thermal properties. © 2015 Wiley Periodicals, Inc. *J. Polym. Sci., Part A: Polym. Chem.* **2015**, *53*, 2421–2430

KEYWORDS: biodegradable; iodine; oxime; polyesters; X-ray

INTRODUCTION Biomedical imaging technologies can be used for both diagnostic and therapeutic purposes, thus making imaging science a critical part of the success of a patient treatment plan in the applied clinical setting. The technologies that find broad use are generally either non- or minimally invasive,^{1–19} and among those, X-ray and computed tomography (CT) imaging are the most common and broadly available. Many of the currently utilized X-ray and CT imaging agents are injectable small molecules with covalently bound iodine that allow for high X-ray attenuation but only when the contrast molecule is in locally high concentration. Nonetheless, these small molecules suffer from non-specific and not easily defined residence in the blood pool and tissues, and experience rapid clearance from circulation. Also, they often have to be administered in high doses to produce significant imaging capability. Our research aims to overcome these limitations by covalently bonding iodine-bearing species onto copolymers through postpolymerization reactions as a new design for biodegradable X-ray contrast

materials, whether for circulation in the body or in implantable devices.

There are many parallel strategies being undertaken to address the challenge of preparing well-defined X-ray opaque materials that have controllable and/or predictable biodistribution. Some current investigations include the "packaging" of the contrast agent as separate small molecules within stabilized organic structures including conventional liposomes, micelles, and emulsions.^{20–25} Unfortunately, these methods of imparting contrast to the material can still suffer from the "leakage" of the contrast agent from the material over time. Other strategies have focused on the covalent attachment of iodine or iodine-containing molecules to the polymer chains, particles, or matrix.^{26–32} Various polymeric structures and architectures such as dendrimers, linear, block, graft, and hyperbranched polymers are also being investigated. These materials can differ in the placement of the radiolabels, with some having the contrast within main chain/backbone of the polymer,^{33–37} at the chain end,³⁸ or as a side group on the

Additional Supporting Information may be found in the online version of this article.

© 2015 Wiley Periodicals, Inc.

monomer^{39,40} or grafted unit. However, there are limited reports of fully biocompatible and biodegradable materials with sufficient X-ray opacity to meet the clinical need of the imaging community.^{32,35,41–44} Our approach seeks to achieve a functional X-ray opaque material that is biodegradable and biocompatible from a combination of copolymerization and postpolymerization reactions. For this reason, we turned our attention to aliphatic polyesters as our polymeric backbone of choice.

Aliphatic polyesters like poly(ϵ -caprolactone), poly(glycolic acid), and poly(lactic acid) have demonstrated biocompatibility and biodegradability and continue to be a standard polymer backbone for drug delivery systems and other biomedical applications.^{45,46} Nevertheless, one major limitation to polyester systems is the fact that the ring-opening polymerizations of the commercially available lactones and lactides normally result in polymers that are not functional and cannot be easily modified. This drawback can be combated with the incorporation of a second monomer via a copolymerization strategy.^{47–56} By using the simple lactone along with another functional lactone, the polyester system becomes a scaffold onto which many different types of small molecules can be attached through postpolymerization, as depicted in Figure 1. It is the goal of this research to present a new type of X-ray opaque material that is (1) quickly synthesized, (2) modular, and (3) inherently biodegradable.

Many methodologies are being employed for postpolymerization modification, with “Click” chemistries of all types receiving significant attention. These reactions meet the criteria of being (1) modular (as in able to work on a variety of substrates and without much ligand specificity), (2) high-yielding, (3) produce harmless side products, and (4) are attainable with mild reaction conditions. Oxime chemistry has broad application as a “Click” reaction in biomolecule conjugation due to its favorable reaction kinetics and thermodynamics under near physiological conditions. It is also a promising polymer conjugation reaction with many examples appearing in the recent synthetic polymer literature, some of which utilize polyester backbones.^{57–75} This versatility is exploited in our work in the preparation of ketone-functionalized polyesters capable of reacting with hydroxylamines to provide a covalent linkage between the polymer and contrast agent. Our interest in the oxime conjugation partly stems from the synthetic simplicity in preparing aminoxy derivatives, including the desired *O*-(2-iodobenzyl) hydroxylamine used to impart the desired X-ray opacity, while maintaining the biodegradability and potentially the biocompatibility of the polyester material itself. Herein, we describe our syntheses and subsequent conjugation of the iodinated species to create a functional copolymer. Furthermore, we provide characterization of the structure, size, and thermal properties of a novel proposed X-ray opaque material with inherent biodegradability.

EXPERIMENTAL

Materials

Meta-chloroperoxybenzoic acid (*m*-CPBA), 1,4-cyclohexanone monoethylene ketal, 2-iodobenzylbromide, *N*-hydroxyl-

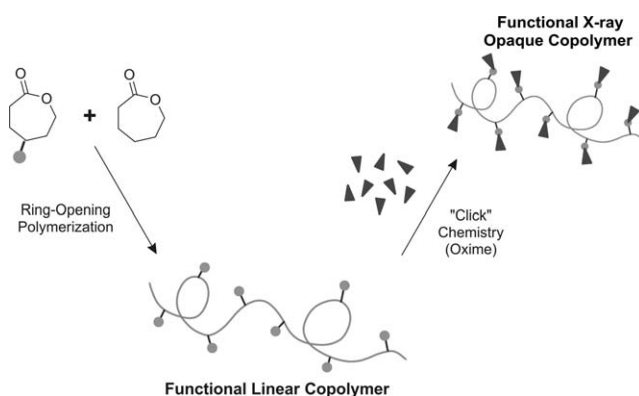


FIGURE 1 General postpolymerization strategy for functionalized copolymers.

phthalimide, triethylamine, and hydrazine monohydrate were purchased from Sigma Aldrich and used as received. Anhydrous sodium sulfate, sodium bisulfite, and sodium bicarbonate were purchased from Fisher Scientific and used as received. Toluene (Sigma Aldrich) was dried by heating at reflux over sodium and distilled under nitrogen prior to use. All other solvents (ethyl acetate, hexanes, methanol (MeOH), dichloromethane (CH₂Cl₂), deuterated chloroform (CDCl₃), and tetrahydrofuran (THF)) were used as received. ϵ -Caprolactone (CL, Sigma Aldrich) and benzyl alcohol (BnOH, Sigma Aldrich) were distilled from calcium hydride (CaH₂) and stored under nitrogen prior to use. Tin (II) 2-ethylhexanoate (Sn(Oct)₂, Sigma Aldrich) was stored over 4–6 Å molecular sieves prior to use. *Para*-toluenesulfonic acid monohydrate (TsOH, Sigma Aldrich) was dissolved in THF to afford a 0.02 M solution.

Instrumentation and Measurements

Proton and carbon nuclear magnetic resonance (¹H and ¹³C NMR) spectroscopy experiments were conducted using a 300 MHz Varian Mercury 300 Vx NMR spectrometer. Samples were acquired in deuterated chloroform for nt=32 or 128 for proton and nt=1024 or 4096 for carbon experiments of small molecules and polymers, respectively. Basic processing and storage were achieved on a Sun Microsystems workstation. NMR figures were generated using Spinworks freeware to process the FID and then exported for plotting using Origin 7.0.

GPC data were acquired on a Malvern GPCMax equipped with an external column heater (35 °C) and Viscotek refractive index detector (VE3580) using inhibited THF as an eluent. Samples were prepared at 1.0 mg/mL in THF and filtered through 0.2 μm PTFE syringe filters (VWR International). Separation was achieved through use of the following columns in series: Malvern (CLM3008-Tguard) Organic Guard Column (10 mm x 4.6 mm), Waters Styragel HR 4ETHF, and Malvern (T6000M) General Mixed Bed (300 mm x 7.8mm) over a 40 minute sample run with molecular weights and polydispersity calculated from a third-order calibration curve from twelve different polystyrene standards M_p ranging from 1050–3.8x10⁶ Da.

IR spectra were recorded on Bruker Alpha FT-IR spectrometers using Opus 6.5 software.

Differential Scanning Calorimetry (DSC) experiments were conducted on a Perkin Elmer DSC 7 over a range of -20 to 180 °C at 5 °C per minute. The data were then processed using the Pyris software to obtain T_m values. Thermogravimetric Analysis (TGA) was performed on a TA Instruments Hi-Res TGA 2950 thermogravimetric analyzer by running samples from 20 to 600 °C at 10 °C per minute under nitrogen.

X-ray imaging was performed using a Tingle 325MVET x-ray machine with 51 kVp, 300 mA, and 5 millisecond exposure time. X-ray samples were prepared from ~ 10 mg each of a control sample of polylactide (PLA), the synthesized P(CL-co-OPD) copolymer, **5a**, and its corresponding functionalized copolymer, **6a**, where the iodine content of the polymer is calculated to be 11.4 weight % iodine after conjugation. PLA was selected as a control because it is commonly used for biomedical applications and does not have radio-opaque properties.

Synthesis

1,4,8-Trioxaspiro[4.6]-9-undecanone (**1**, TOSUO)

[This procedure is a modification of the synthesis originally reported.⁷⁶⁻⁷⁹] 1,4-cyclohexanedione monoethylene acetal (4.99 g, 32.0 mmol, 1.0 eq.) was dissolved in methylene chloride (50 mL) in a 300 mL RBF and was allowed to stir for 10 minutes. *Meta*-chloroperoxybenzoic acid (11.50 g, 48.0 mmol, 1.5 eq.) was added to the flask in scoops to the 300 mL round bottom flask over 30 minutes. A white precipitate was noted approximately 20 minutes after all reagents had been added. The reaction was allowed to proceed with stirring at room temperature overnight. The contents of the reaction flask were added to a 1000 mL Erlenmeyer flask equipped with a stirbar, followed by 100 mL of H₂O and 50 mL of CH₂Cl₂. Sodium bisulfite (7.67 g) was then added to the stirring mixture over 30 minutes, followed by sodium bicarbonate (6.82 g), and allowed to stir overnight. The contents of the Erlenmeyer were then poured into a 2 L separatory funnel where the organics were collected. The aqueous layer was washed with 2 x 50 mL of CH₂Cl₂. The combined organic layers were then extracted with 2 x 50 mL of sodium bisulfite solution, 2 x 50 mL of saturated sodium bicarbonate solution, and 1 x 100 mL of brine. The organic layer was then dried over anhydrous sodium sulfate and concentrated by rotary evaporation to yield a viscous off-white oil that became a crystalline white solid under high vacuum. Yield: 4.91 g (89 %) ¹H NMR (300 MHz, CDCl₃, δ): 4.25 (m, 2 H, -COOCH₂-), 3.94 (s, 4H, acetal -OCH₂CH₂O-), 2.67 (m, 2H, -COCH₂-), 1.98 (m, 2H, -COOCH₂CH₂-), 1.87 (m, 2H, -COCH₂CH₂-); ¹³C NMR (75 MHz, CDCl₃, δ): 175.7 (C=O), 108.1 (ketal), 65.0, 64.6, 39.3, 32.9, 29.1 ppm.

O-(2-iodobenzyl)-*N*-hydroxyphthalimide by Nucleophilic Substitution from 2-iodobenzyl Bromide (**2**)

N-hydroxyphthalimide (2.86 g, 17.53 mmol, 1.3 eq.) was added to a 500 mL round bottom flask using a solids funnel

followed by 45 mL of THF. Triethylamine (2.8 mL, 20.1 mmol, 1.5 eq.) was added to the reaction flask using a 5 mL syringe and a red color was immediately observed upon addition. A stock solution of 2-iodobenzyl bromide (3.97 g, 13.4 mmol, 1.0 eq.) in THF (15 mL) was added dropwise to the reaction round bottom flask in 3 aliquots of 5 mL. The flask was capped and the reaction was allowed to proceed at room temperature for 18 h. The crude reaction mixture was characterized with TLC using a 1:1 hexanes:ethyl acetate eluent. After removal of the THF solvent by rotary evaporation, the reaction mixture contents were transferred into a separatory funnel by rinsing of the round bottom flask with methylene chloride (165 mL) and water (165 mL). After initial separation, the organic layer was set aside and the aqueous layer was extracted 2 x 100 mL of CH₂Cl₂. The organic layers were combined and then washed with distilled water (3 x 100 mL) and once with brine (100 mL). The combined organic layer was then dried over anhydrous sodium sulfate in a 500 mL Erlenmeyer overnight. The organic layer was filtered the following day and concentrated by rotary evaporation and high vacuum to yield an off-white powdery solid. No further purification by column chromatography was required. Yield: 4.72 g (93 % isolated). ¹H NMR (300 MHz, CDCl₃, δ): 7.92 (m, 1H, Ar **H**), 7.90 (m, 1H, phthalimido), 7.78 (m, 1H, phthalimido), 7.61 (d, 1H, Ar **H**), 7.48 (t, 1H, Ar **H**), 7.01 (t, 1H, Ar **H**), 5.35 (s, 2H, C₆H₄ICH₂-) ppm. ¹³C NMR (75 MHz, CDCl₃, δ): 163.6 (phthalimide), 139.8, 137.1, 134.7, 131.4, 130.1, 129.1, 129.7, 123.8, 99.8, 83.1 ppm; IR (solid, ATR): $\nu = 3057$ (w), 2962-2854 (w), 1783 and 1723 (vs, broad over range to 1650), 1618 (w), 1607 (w), 1586 (w) 1462 (m), 1439 (m), with fingerprint peaks at 1387, 1370, 1354, 1183, 1128, 1102, 1079, 1011, 967, 875 cm⁻¹.

O-(2-iodobenzyl) Hydroxylamine (**3**)

O-(2-iodobenzyl)-*N*-hydroxyphthalimide (0.50 g, 1.32 mmol, 1.0 eq.) was massed into a 100 mL round bottom flask equipped with a stirbar. To this flask, THF (15 mL) was added and the mixture was allowed to stir for 15 minutes to dissolve the starting material. Hydrazine monohydrate (0.35 mL, 7.2 mmol, 5.5 eq.) was then added by syringe to the reaction and a light yellow color change was observed. The reaction was allowed to proceed for 24 h at room temperature. Next, the reaction mixture (murky white) was washed twice with water, once with brine, and once with methylene chloride. The mixture was purified by column chromatography with methylene chloride as eluent (increasing polarity with methanol as needed) and concentrated by rotary evaporation to afford an off-white oil. Yield: 0.32 g (97% isolated). ¹H NMR (300 MHz, CDCl₃, δ): 7.81 (d, 1H, Ar **H**), 7.35-7.49 (m, 2H, Ar **H**), 7.0 (t, 1H, Ar **H**), 6.51 (broad s, 2H, -ONH₂), 4.69 (s, 2H, C₆H₄ICH₂-) ppm; ¹³C NMR (75 MHz, CDCl₃, δ) 139.9, 139.7, 129.8, 128.5, 99.1, 81.7 ppm; IR (from CDCl₃ solution): $\nu = 3309$ and 3235 (m, broad), 3146 (w), 3059 (w) 2920 and 2867 (w, broad), 1584, 1563, 1464, and 1436 (m), with fingerprint peaks at 1272, 1184, 1109, 1045, 1006, 944, 900, 745, 648 cm⁻¹.

Example Procedure for Conventional Ring-opening Polymerization Using CL, TOSUO, Sn(Oct)₂, and Benzyl Alcohol to Afford Poly(CL₇₁-co-TOSUO₁₁) (4a)

Dry CL (6.6 mL, 60 mmol, 90 eq.) and TOSUO (**3**) (1.19 g, 6.9 mmol, 10 eq.; from a 2.0 M dry toluene solution) were added to a 100 mL 3-neck round bottom flask equipped with a stirbar using dry syringes and needles. An additional 4 mL of dry toluene was added to the reaction flask under inert N₂ atmosphere, followed by distilled benzyl alcohol (70 μL, 0.66 mmol, 1.0 eq.) and tin (II) octanoate catalyst (110 μL, 0.34 mmol, 0.51 eq.). The bottom of the flask was submerged in a silicone oil bath with the temperature set to maintain 110 °C. Reaction was monitored by removal of an aliquot for ¹H NMR analysis at 18 h and was subsequently quenched with 2 drops of TsOH (0.2 M in THF). The reaction mixture was precipitated in 1500 mL of cold methanol to yield white solid that was collected on a fritted funnel and dried under vacuum. Yield: 6.72 g (87% overall yield as measured from 96% conversion of ε-CL and 94% conversion of TOSUO by ¹H NMR of the crude reaction mixture). Confirmed final product as poly(CL₇₁-co-TOSUO₁₁). ¹H NMR (300 MHz, CDCl₃, δ): 7.35–7.4 (m, 5H, Ar **H**), 5.12 (s, 2H, benzylic **H** of end group), 4.15 (m, 2H, -CH₂OCO- TOSUO), 4.05 (t, 2H, -CH₂OCO- CL), 3.95 (s, 4H, -OCH₂CH₂O- TOSUO ketal), 3.65 (t, 2H, -CH₂OH end group), 2.39 (t, 2H, -OCOCH₂- TOSUO), 2.30 (t, 2H, -OCOCH₂- CL), 2.05–1.90 (m, 4H, -OCOCH₂CH₂C(OCH₂CH₂O)CH₂CH₂O- TOSUO), 1.60 (m, 4H, -OCOCH₂CH₂CH₂CH₂CH₂O- CL), 1.40 (m, 2H, -OCOCH₂CH₂CH₂CH₂CH₂O- CL) ppm. ¹³C NMR (75 MHz, CDCl₃, δ) 173.8, 173.6, 128.8, 128.4, 109.6, 77.5 (not CDCl₃) 65.3, 64.5, 64.3, 62.7, 60.5, 60.4, 36.2, 34.4, 34.3, 32.8, 32.5, 28.9, 28.8, 28.5, 25.7, 25.5, 24.9, 24.8, 24.7 ppm; T_{m, DSC} = 44.7 °C (range 40.1–46.3 °C)

Example Procedure for the Polymeric Ketal Deprotection Using Trityltetrafluoroborate to Afford of Poly(CL₇₁-co-OPD₁₁) (5a)

P(CL₇₁-co-TOSUO₁₁) (1.98 g, 0.196 mmol, 1.0 eq. of polymer with 11.0 eq. of ketone) was transferred into a 500 mL round bottom flask followed by 200 mL of CH₂Cl₂. Trityltetrafluoroborate (0.94 g, 2.8 mmol, 1.3 eq. per ketone) was added to the stirring flask and a bright yellow/orange color was observed. The reaction was allowed to proceed for 1 h. The reaction mixture was added by pipette into 1500 mL of ice cold methanol and allowed to stir for > 3 h. The white solid product was isolated over a fritted funnel and dried with vacuum. Yield: 1.40 g. (74% isolated) ¹H NMR (300 MHz, CDCl₃, δ): 7.35–7.4 (m, 5H, Ar **H** end group), 5.12 (s, 2H, benzylic **H**), 4.35 (m, 2H, -CH₂OCO- OPD), 4.05 (t, 2H, -CH₂OCO- CL), 3.65 (t, 2H, -CH₂OH end group), 2.80–2.75 (two t, 4H, OCOCH₂CH₂COCH₂CH₂O- OPD), 2.39 (t, 2H, -OCOCH₂- OPD), 2.30 (t, 2H, -OCOCH₂- CL), 1.60 (m, 4H, -OCOCH₂CH₂CH₂CH₂CH₂O- CL), 1.40 (m, 2H, -OCOCH₂CH₂CH₂CH₂CH₂O- CL) ppm. ¹³C NMR (75 MHz, CDCl₃, δ) 206.0, 173.7, 173.5, 172.9, 128.8, 128.4, 77.5 (not CDCl₃), 64.7, 64.3, 62.7, 59.4, 59.3, 41.7, 37.6, 34.3, 34.1, 33.6, 32.5, 28.54, 28.47, 28.0, 25.72, 25.67, 25.5, 24.8 24.6 ppm; T_{m, DSC} = 57.1 °C (range 55.4–58.4 °C)

Example Procedure for the Oxime “Click” Reaction of *O*-(2-iodobenzyl)hydroxylamine onto P(CL₇₁-co-OPD₁₁) to Afford Functionalized Copolymer P(CL₇₁-co-(OPD-mod-(2-IBn))₁₁) (6a)

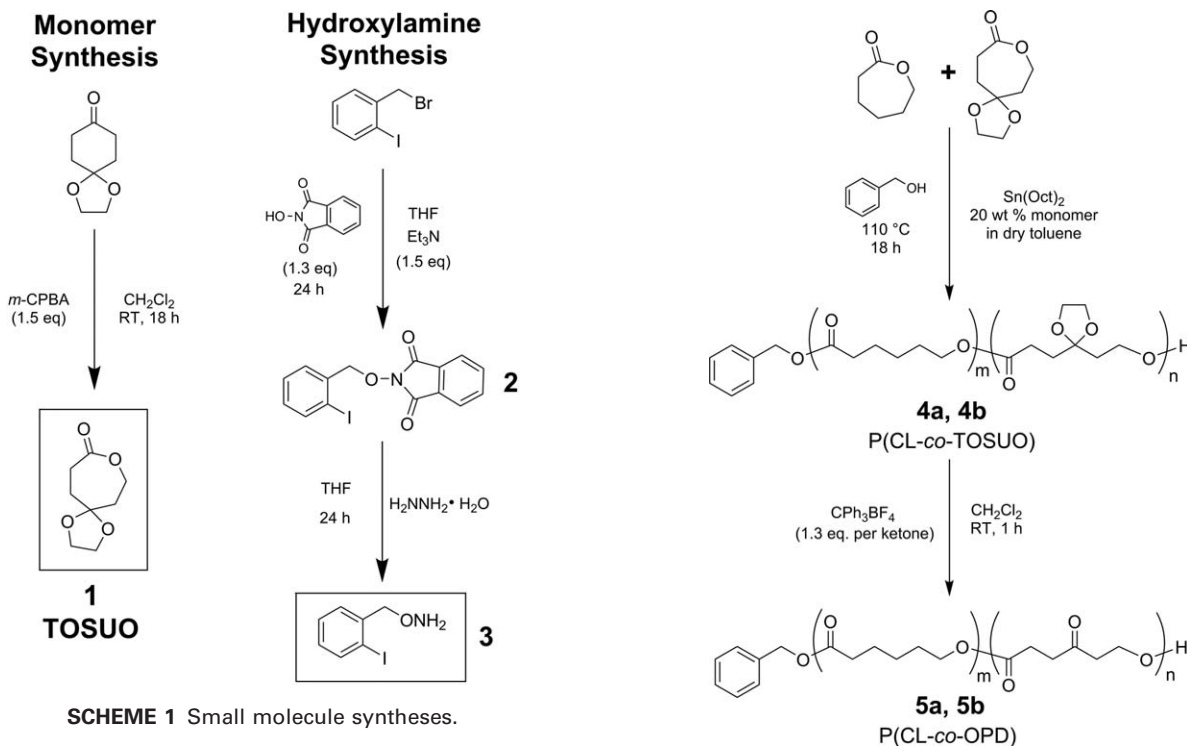
P(CL₇₁-co-OPD₁₁) polymer (0.203 g, 0.021 mmol polymer containing 0.23 mmol ketone) was massed into a scintillation vial equipped with a stirbar and to it was added 3 mL of THF. A 10 mL stock solution of *O*-(2-iodobenzyl) hydroxylamine (0.10 M) was prepared in a different vial and 2.35 mL of hydroxylamine stock were subsequently delivered by syringe to the reaction vial. Three drops of a THF stock solution of TsOH (0.02 M) were added to the reaction vial and the reaction was allowed to proceed with stirring for 24 h at room temperature. The contents of the vial were then precipitated into 300 mL cold hexanes, followed by collection by filtration and drying under vacuum. Yield: 0.177 g (79% isolated) Abbreviated as P(CL₇₁-co-(OPD-mod-(2-IBn))₁₁) ¹H NMR (300 MHz, CDCl₃, δ): 7.83–7.81 (dd, 1H, Ar **H3**), 7.4–7.35 (m, 5H, Ar **H** end group), 7.35–7.31 (dd and td, 2H, Ar **H3** & **H5**), 6.98 (td, 1H, Ar **H4**), 5.12 (s, 2H, benzylic **H**), 5.1 (d, 2H, -CH₂ON- oxime), 4.27 (m, 2H, -CH₂OCO- oxime), 4.05 (t, 2H, -CH₂OCO- CL), 3.65 (t, 2H, -CH₂OH end group), 2.70–2.45 (three t, 6H, OCOCH₂CH₂C(oxime)CH₂CH₂O- OPD), 2.30 (t, 2H, -OCOCH₂- CL), 1.60 (m, 4H, -OCOCH₂CH₂CH₂CH₂CH₂O- CL), 1.40 (m, 2H, -OCOCH₂CH₂CH₂CH₂CH₂O- CL) ppm. ¹³C NMR (75 MHz, CDCl₃, δ) 173.8, 173.5, 172.9, 157.1, 156.3, 140.5, 139.5, 139.4, 129.52, 129.48, 128.3, 98.2, 98.1, 79.5, 64.8, 64.4, 34.3, 34.2, 34.0, 30.5, 28.6, 25.8, 24.8 ppm; T_{m, DSC} = 37.4 and 42.7 °C (range 26.9–44.1 °C)

RESULTS AND DISCUSSION

Small Molecule Syntheses of Monomer and Iodinated Hydroxylamine

To allow for the additional chemical functionality to be imparted to the polyester material, we chose to use a copolymerization and postpolymerization strategy. Our devised route employs a previously published monomer, 1,4,8-trioxaspiro[4.6]-9-undecanone (abbreviated TOSUO, **1**) which is prepared from the Baeyer-Villiger oxidation of 1,4-cyclohexanedione monoethylene acetal. This functional monomer has been reported previously to copolymerize with CL^{77–80} and was utilized in our desired polymer syntheses.

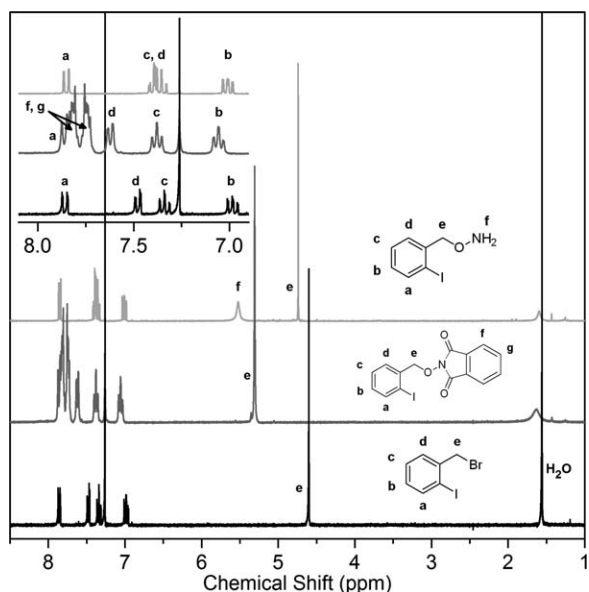
The preparation of the iodine-containing hydroxylamine was achieved through the nucleophilic substitution of 2-iodobenzyl bromide by *N*-hydroxyphthalimide in the presence of triethylamine also shown in Scheme 1. The removal of phthalimido group was accomplished by exposing the phthalimido derivative, **2**, to hydrazine overnight at room temperature to yield a final product of *O*-(2-iodobenzyl) hydroxylamine, **3**, after a short column purification. Both the purified *O*-(2-iodobenzyl)-*N*-hydroxyphthalimide, **2**, and final *O*-(2-iodobenzyl) hydroxylamine, **3**, were characterized by ¹H and ¹³C NMR spectroscopies, which confirmed the disappearance of the second aromatic resonances and shifting of the benzylic methylene unit adjacent to the hydroxylamine as visualized in the proton NMR spectrum and aromatic inset



of Figure 2. Infrared spectroscopy also confirmed the structures with carbonyl absorbances at 1783 and 1723 cm^{-1} indicative of the phthalimido group that were then absent in the hydroxylamine, where additional N-H stretches at 3309 and 3235 cm^{-1} were observed.

Polymer Synthesis and Ketal Deprotection

Traditional ring-opening polymerization with tin (II) octanoate was employed to create copolymers with a predictable incorporation of comonomer, as represented in the Scheme 2.



SCHEME 2 Ring-opening polymerization, deprotection, and functionalization reactions.

This copolymerization of CL and TOSUO was achieved using benzyl alcohol as the initiator in dry toluene at 20 weight percent monomer at 110 $^{\circ}\text{C}$ for 18 h. The reaction was monitored with ^1H NMR spectroscopy by calculating the percent conversion of monomer to polymer with the methylene unit ratios on the oxygen side of the ester with measured conversions $> 90\%$ for all polymerizations. The final products were isolated from precipitation in methanol non-solvent, dried under vacuum and then characterized with ^1H NMR spectroscopy to determine a percent TOSUO incorporation and a number average molecular weight as tabulated in Table 1. Subsequent removal of the ketal units was achieved using trityltetrafluoroborate in dichloromethane, followed by precipitation in methanol, and isolation and drying of the solid product to yield poly(caprolactone-co-1,4-oxepan-1,5-dione), abbreviated P(CL-co-OPD). Figure 3 provides representative ^1H NMR spectra of purified samples **4b** and **5b** with the incorporation of TOSUO monomer calculated at 17.0 mol% as P(CL₇₈-co-TOSUO₁₆) and its corresponding P(CL₇₈-co-OPD₁₆)

TABLE 1 Proton NMR and GPC Characterization of Copolymers and Modified Copolymers

Polymer Sample	CL Repeat Units ^a	Functional Repeat Units ^a	Mole % Functionality	M _n , NMR ^a	M _n , GPC ^b	M _w , GPC ^b	PDI ^b
4a P(CL-co-TOSUO)	71	11	13.1	10100	10800	17300	1.60
5a P(CL-co-OPD)	71	11	13.1	9620	13200	17900	1.36
6a Iodine Modified Copolymer	71	11	13.1	12200	13600	18400	1.35
4b P(CL-co-TOSUO)	78	16	17.0	11800	19000	29200	1.54
5b P(CL-co-OPD)	78	16	17.0	11100	18900	27800	1.47
6b Iodine Modified Copolymer	78	16	17.0	14800	19900	28400	1.43

^a Calculated from ¹H NMR spectra using the ratio of the -COOCH₂-methylene integrations of CL and TOSUO repeat units in the polymers and the benzylic methylene end group after isolation from MeOH precipitation.

^b GPC data acquired with a Malvern GPCMax with an RI detector and PS standards from single runs on same day.

deprotected ketone polymer daughter product. These spectra confirm the complete removal of the ethylene glycol units and shifting of the methylene units alpha to the ketones. Additionally, ¹³C NMR spectroscopy established the presence of ketone units at 206 ppm in the OPD polymer and the disappearance of the spiroketal carbon at 109.6 ppm after the deprotection step.

Postpolymerization Modification via Acid-catalyzed Oxime Chemistry

Attachment of the newly synthesized *O*-(2-iodobenzyl) hydroxylamine to the P(CL-co-OPD) polymer backbones was achieved through *p*-toluene sulfonic acid-catalyzed oxime formation in THF solution, followed by precipitation into cold methanol, isolation by filtration, and drying under vacuum to yield a white solid graft copolymer. To demonstrate the reproducibility and effective matching of reaction mixture and polymer product stoichiometries, each of the ketone-bearing polymers (**5a** and **5b**) was exposed to 1.1 equiva-

lents of hydroxylamine per ketone under the conditions listed above.

Proton NMR spectroscopy confirmed that ~100% coupling was achieved on both samples (Products **6a** and **6b**) as can be seen by the complete shifting of the two different methylene subunits alpha to the ketone (from b', d' to b'', d'') to new positions in the oxime product in Figure 4 along with a shift in the methylenes (from e' to e'') adjacent to the oxygen of the backbone ester groups. Additionally, new benzylic methylene resonances (f'') appear at 5.1 ppm. These NMR results provide evidence of a well-defined and controllable coupling reaction stoichiometry as observed through characterization of the final products. ¹³C NMR also indicated attachment of the hydroxylamine through the appearance of new aromatic resonances from 99–140 ppm, appearance of a pair of oxime isomer resonances at 156.3 and 157.1 ppm, as well as the disappearance of the C=O resonance at 206 ppm. The GPC overlay in Figure 5 and data tabulated in

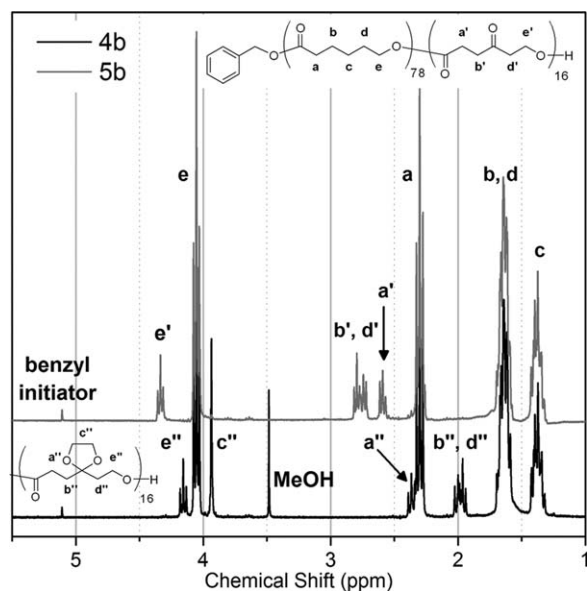


FIGURE 3 ¹H NMR spectral overlay of polymer deprotection of P(CL-co-TOSUO) **4b** to yield P(CL-co-OPD) **5b**.

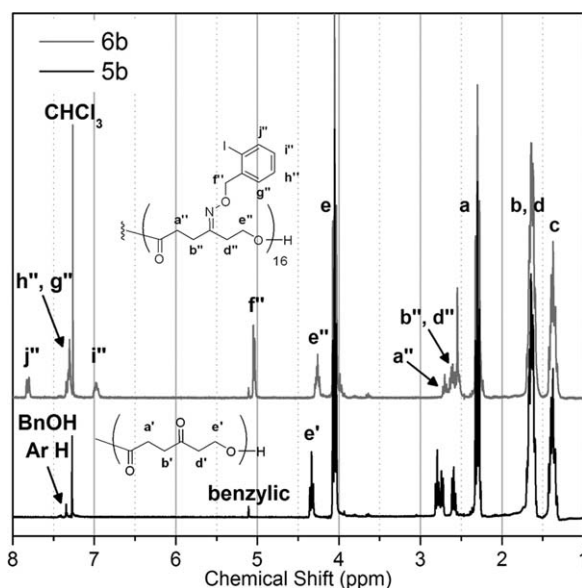


FIGURE 4 ¹H NMR comparison of P(CL-co-OPD) **5b** and P(CL-co-(OPD-mod-(2-IBn))) **6b**.

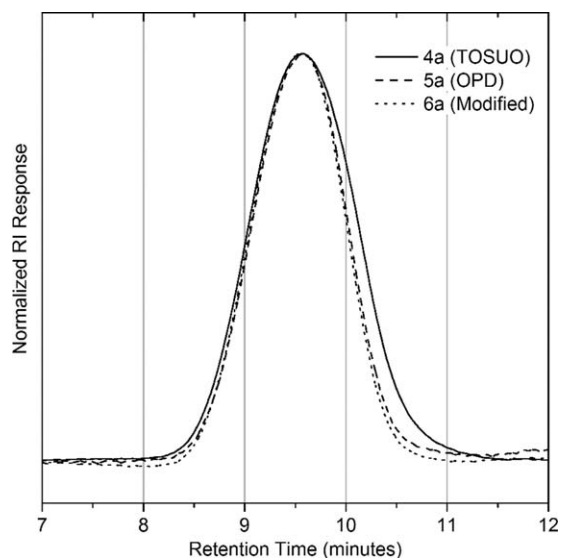


FIGURE 5 Overlay of GPC curves of copolymers.

Table 1 of the **4a**, **5a**, and **6a** products confirm that no unwanted degradation of the polymer backbone was observed during the 24 h exposure to the acid catalyst. Additionally, no dramatic change in the molecular weight distribution or peak molecular weight of the chromatogram for the modified copolymer was observed relative to the ketone-bearing and ketal-containing polymer precursors. These NMR and GPC results support our claim of the stability of the polymer under varying reaction conditions and the efficiency and accuracy of the polymer oxime reaction for creating iodinated poly(ϵ -caprolactone) materials.

Thermal Analysis of Copolymers and Graft Copolymers with DSC and TGA

Given the influence of thermal stability and crystallinity on the potential *in vivo* degradation of the synthetic iodine-

modified PCL material, thermal analysis by differential scanning calorimetry (DSC) was performed on each of the polymer precursors and the final products. As expected, both the P(CL-co-TOSUO) initial copolymer **4a** and the oxime graft product **6a** display lower melting transition temperatures [Fig. 6(a)] than unfunctional pure PCL ($T_m \sim 60^\circ\text{C}$) while the P(CL-co-OPD) **5a** melts at higher temperatures. These results are expected due to the disruption of the crystalline packing of the polymers arising from the spiroketal and bulky aromatic side chains on the P(CL-co-TOSUO) and oxime graft product, respectively, and the increased regular packing and improved crystalline structure with the intermediate ketone-bearing OPD polymer.^{81–83} The lower T_m range ($35^\circ\text{C} > T_m > 50^\circ\text{C}$) for the final graft copolymers is particularly interesting since a material T_m near physiological temperatures could have a significant impact on the material degradation *in vivo*.

To learn more about how the compositional and structural changes of the oxime conjugated copolymer affect the thermal stability of the system, thermogravimetric analysis (TGA) was performed. Main chain PCL degradation and depolymerization were observed for the OPD and oxime copolymers at temperature $\geq 400^\circ\text{C}$ as expected while the starting ketal copolymers degraded as a whole at significantly lower temperatures, as depicted in Figure 6(b). Interestingly, we did not observe much of an early thermal degradation mode for the P(CL-co-OPD) polymers such as **5a** in the $150\text{--}250^\circ\text{C}$ region. This degradation mode is believed to represent the β -elimination mechanism resulting from the methylenes adjacent to the ketone or oxime units. Degradation of this type has been previously documented for ketone-containing polymer systems⁸¹ as well as oxime-modified polymers, and begins at temperatures as low as 150°C . For the oxime-modified copolymers (see **Supporting Information Figure S1** - derivative plot and Figure 6(b)), including polymer **6a**, a substantial mass loss was detected and peaked at about

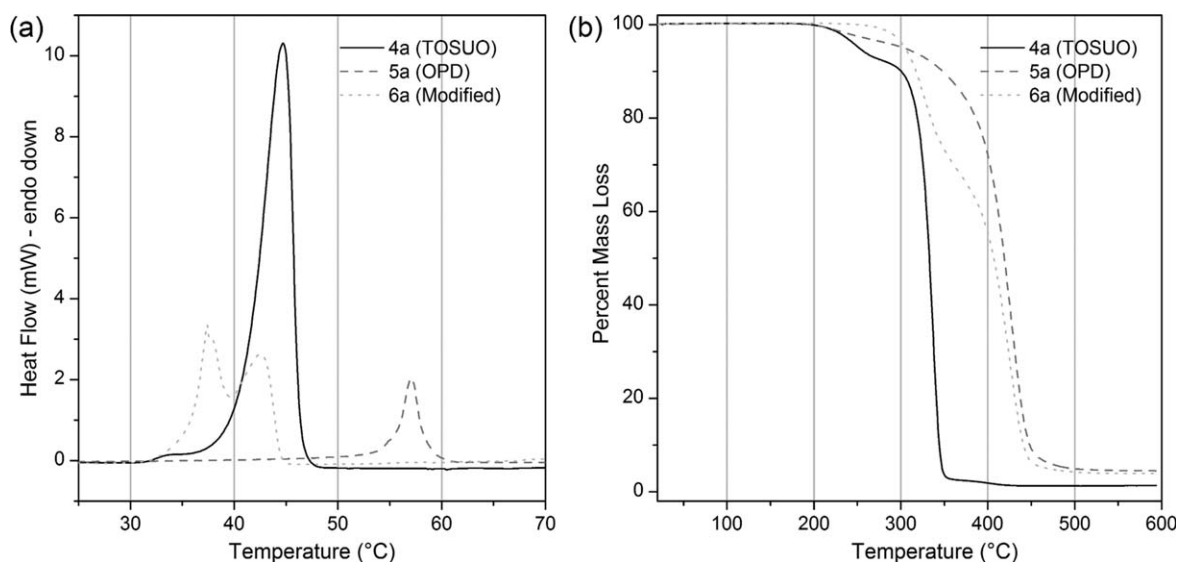


FIGURE 6 Thermal analysis of copolymers with (a) DSC and (b) TGA.

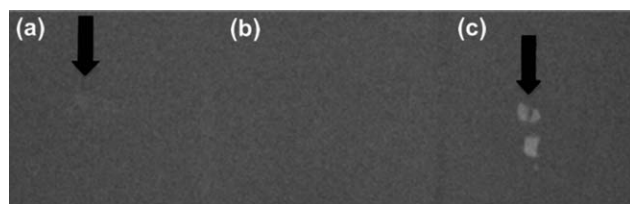


FIGURE 7 Preliminary X-ray analysis of (a) a PLA polymer control, (b) the P(CL-co-OPD) control, 5a, and (c) the oxime-modified sample, 6a using ~ 10 mg samples. X-ray imaging was performed using a Tingle 325MVET x-ray machine with 51 kVp, 300 mA and 5 millisecond exposure time.

325 °C, potentially due to the removal of the oxime-linked benzyl units, which correlates well with ~30% reduction in mass being expected if all OPD-*mod*-OBnI units were cleaved in heating for this sample. These data further confirm the successful covalent attachment of the iodinated benzyl hydroxylamines to the P(CL-co-OPD) polymers.

X-ray Imaging of the Graft Copolymers

The X-ray contrast imaging properties of the functionalized copolymers were then examined. The iodine content of the final copolymers is calculated to be 11.4 and 13.7 weight percent iodine for samples **6a** and **6b**, respectively, assuming that each ketone is modified by the hydroxylamine as the NMR data suggest. These values align with other reports⁸⁴ of the required iodine content to observe X-ray contrast. Figure 7 shows a comparison of a control sample of PLA (a), a 10 mg sample of P(CL-co-OPD), **5a** (b), and a 10 mg sample of functional copolymer, **6a** (c). These preliminary images indicate that sufficient iodinated hydroxylamine has been grafted onto the copolymers to produce visible X-ray contrast.

CONCLUSIONS

In this article, we present one specific direction by which a radio-opaque biodegradable polyester can be achieved, namely through postpolymerization modification of copolymers. The chemistry for attachment of the mono-iodinated molecules took advantage of a versatile, robust, and efficient chemical reaction to form oxime linkages through the reaction of a hydroxylamine and backbone ketone units in the polyester to afford iodine-containing copolymers. This strategy could allow for the creation of variable iodine content materials from one parent polymer, giving the material tunable X-ray opacity. Additionally, this novel polymer system was developed to exploit the biodegradable and biocompatible characteristics of poly(ϵ -caprolactone), both increasingly important priorities for polymer systems to be used *in vivo*. Current⁸⁵ and future studies are planned to address the ability to image the polymer in soft tissues, to examine materials degradation kinetics and by-products, and determine the biocompatibility to more fully understand the biological applications of this promising material.

ACKNOWLEDGMENTS

This work has been supported by multiple College of Charleston sources to provide undergraduate researcher and faculty stipends, supplies, and instrument time. The internal sources include start-up funds, the Department of Chemistry and Biochemistry, and the Undergraduate Research and Creative Activities office (SURF awards including SU2013-011 and SU2013-035; RPGs including RP2013-007, RP2013-010, RP2014-010, and RP2014-017). Additionally, this research was supported in part by Howard Hughes Medical Institute (HHMI) Undergraduate Science Education Grants to the College of Charleston (# 52006290 and #52007537) through four Summer Research Awards. This material is also supported by the National Science Foundation under MRI grant CHE-1229559. We would like to thank Kimberly Ivery (Clemson) for the TGA analysis and the Institute for Biological Interfaces of Engineering (IBIOE) for DSC assistance.

REFERENCES

- 1 K. Yang, L. Z. Feng, X. Z. Shi, Z. Liu, *Chem. Soc. Rev.* **2013**, *42*, 530–547.
- 2 S. Svenson, *Mol. Pharm.* **2013**, *10*, 848–856.
- 3 H. Qi, Y. H. Zhu, H. B. Xu, X. L. Yang, *Prog. Chem.* **2013**, *25*, 611–619.
- 4 D. Pan, *Mol. Pharm.* **2013**, *10*, 781–782.
- 5 H. Lusic, M. W. Grinstaff, *Chem. Rev.* **2013**, *113*, 1641–1666.
- 6 N. Khlebtsov, V. Bogatyrev, L. Dykman, B. Khlebtsov, S. Staroverov, A. Shirokov, L. Matora, V. Khanadeev, T. Pylaev, N. Tsyganova, G. Terentyuk, *Theranostics* **2013**, *3*, 167–180.
- 7 Y. J. Guo, T. Aweda, K. C. L. Black, Y. J. Liu, *Curr. Top. Med. Chem.* **2013**, *13*, 470–478.
- 8 M. Espinoza-Castaneda, A. de la Escosura-Muniz, G. Gonzalez-Ortiz, S. M. Martin-Orue, J. F. Perez, A. Merkoci, *Biosens. Bioelectron.* **2013**, *40*, 271–276.
- 9 G. Y. Chen, G. Han, *Theranostics* **2013**, *3*, 289–291.
- 10 J. K. Young, E. R. Figueroa, R. A. Drezek, *Ann. Biomed. Eng.* **2012**, *40*, 438–459.
- 11 D. Yoo, J. H. Lee, T. H. Shin, J. Cheon, *Acc. Chem. Res.* **2012**, *45*, 1622–1622.
- 12 Y. H. Wang, L. Huang, *Mol. Ther.* **2012**, *20*, 10–11.
- 13 N. Vij, A. Gorde, In *Pulmonary Nanomedicine: Diagnostics, Imaging, and Therapeutics*; Vij, N. Ed.; Pan Stanford Publishing Pte.: Singapore, **2012**; Chapter 1, pp 1–14.
- 14 E. Terreno, F. Uggeri, S. Aime, *J. Control. Release* **2012**, *161*, 328–337.
- 15 A. Singh, T. Chernenko, M. Amiji, In *Functional Nanoparticles for Bioanalysis, Nanomedicine, and Bioelectronic Devices*, Volume 2, Hepel, M. and Zhong, C.-J. Eds.; ACS Symposium Series 1113; American Chemical Society: Washington DC, **2012**, pp 383–413.
- 16 E. B. Silberstein, *Semin. Nucl. Med.* **2012**, *42*, 164–170.
- 17 P. Prabhu, V. Patravale, *J. Biomed. Nanotechnol.* **2012**, *8*, 859–882.
- 18 Y. J. Liu, N. Zhang, *Biomaterials* **2012**, *33*, 5363–5375.
- 19 N. Matsuura, J. A. Rowlands, *Med. Phys.* **2008**, *35*, 4474–4487.

- 20 X. Li, N. Anton, G. Zuber, M. J. Zhao, N. Messaddeq, F. Hallouard, H. Fessi, T. F. Vandamme, *Biomaterials* **2013**, *34*, 481–491.
- 21 F. Hallouard, S. Briancon, N. Anton, X. Li, T. Vandamme, H. Fessi, *Eur. J. Pharm. Biopharm.* **2013**, *83*, 54–62.
- 22 F. Hallouard, N. Anton, G. Zuber, P. Choquet, X. Li, Y. Arntz, G. Aubertin, A. Constantinesco, T. F. Vandamme, *RSC Adv.* **2011**, *1*, 792–801.
- 23 S. Ahn, S. Y. Jung, J. P. Lee, S. J. Lee, *J. Phys. Chem. B* **2011**, *115*, 889–901.
- 24 S. Ahn, S. Y. Jung, J. P. Lee, S. J. Lee, *Contrast Med. Mol. Imaging* **2011**, *6*, 437–448.
- 25 D. Pan, T. A. Williams, A. Senpan, J. S. Allen, M. J. Scott, P. J. Gaffney, S. A. Wickline, G. M. Lanza, *J. Am. Chem. Soc.* **2009**, *131*, 15522–15527.
- 26 N. R. James, J. Philip, A. Jayakrishnan, *Biomaterials* **2006**, *27*, 160–166.
- 27 S. Lakshmi, N. R. James, V. S. Nisha, A. Jayakrishnan, *J. Appl. Polym. Sci.* **2003**, *88*, 2580–2584.
- 28 M. Okamura, T. Yamanobe, T. Arai, H. Uehara, T. Komoto, S. Hosoi, T. Kumazaki, *J. Mol. Struct.* **2002**, *602*, 17–28.
- 29 Y. B. J. Aldenhoff, M. A. B. Kruft, A. P. Pijpers, F. H. van der Veen, S. K. Bulstra, R. Kuijter, L. H. Koole, *Biomaterials* **2002**, *23*, 881–886.
- 30 S. Dawlee, M. Jayabalan, *J. Appl. Polym. Sci.* **2012**, *125*, 2252–2261.
- 31 S. Dawlee, M. Jayabalan, *Biomed. Mater.* **2011**, *6*, 12.
- 32 M. D. Hindenlang, A. A. Soudakov, G. H. Imler, C. T. Laurencin, L. S. Nair, H. R. Allcock, *Polym. Chem.* **2010**, *1*, 1467–1474.
- 33 C. Rode, A. Schmidt, R. Wyrwa, J. Weisser, K. Schmidt, N. Moszner, R. P. Gottlober, K. Heinemann, M. Schnabelrauch, *Polym. Int.* **2014**, *63*, 1732–1740.
- 34 L. Sang, Z. Y. Wei, K. L. Liu, X. H. Wang, K. D. Song, H. Wang, M. Qi, *J. Biomed. Mater. Res. Part A* **2014**, *102*, 1121–1130.
- 35 S. Kiran, N. R. James, A. Jayakrishnan, R. Joseph, *J. Biomed. Mater. Res. Part A* **2012**, *100A*, 3472–3479.
- 36 S. Kiran, R. Joseph, *J. Biomed. Mater. Res. Part A* **2014**, *102*, 3207–3215.
- 37 Q. Yin, F. Y. Yap, L. C. Yin, L. Ma, Q. Zhou, L. W. Dobrucki, T. M. Fan, R. C. Gaba, J. J. Cheng, *J. Am. Chem. Soc.* **2013**, *135*, 13620–13623.
- 38 H. W. Kao, C. J. Chan, Y. C. Chang, Y. H. Hsu, M. Lu, J. S. J. Wang, Y. Y. Lin, S. J. Wang, H. E. Wang, *Appl. Radiat. Isot.* **2013**, *80*, 88–94.
- 39 Z. Y. Wang, T. Chang, L. Hunter, A. M. Gregory, M. Tanudji, S. Jones, M. H. Stenzel, *Aust. J. Chem.* **2014**, *67*, 78–84.
- 40 S. Li, J. Yu, M. B. Wade, G. M. Policastro, M. L. Becker, *Biomacromolecules* **2015**, *16*, 615–624.
- 41 A. L. Carbone, M. Song, K. E. Uhrich, *Biomacromolecules* **2008**, *9*, 1604–1612.
- 42 B. Nottelet, J. Coudane, M. Vert, *Biomaterials* **2006**, *27*, 4948–4954.
- 43 S. El Habnoui, V. Darcos, J. Coudane, *Macromol. Rapid Comm.* **2009**, *30*, 165–169.
- 44 S. El Habnoui, S. Blanquer, V. Darcos, J. Coudane, *J. Polym. Sci., Part A: Polym. Chem.* **2009**, *47*, 6104–6115.
- 45 M. A. Woodruff, D. W. Hutmacher, *Prog. Polym. Sci.* **2010**, *35*, 1217–1256.
- 46 F. Alexis, *Polym. Int.* **2005**, *54*, 36–46.
- 47 J. Hao, E. A. Rainbolt, K. Washington, M. C. Biewer, M. C. Stefan, *Curr. Org. Chem.* **2013**, *17*, 930–942.
- 48 P. Lecomte, C. Jerome, In *Synthetic Biodegradable Polymers*, B. Rieger, A. Kunkel, G. W. Coates, R. Reichardt, E. Dinjus, T. A. Zevaco, Eds.; Springer-Verlag Berlin: Berlin, **2012**; Vol. *245*, pp 173–217.
- 49 H. Kim, J. V. Olsson, J. L. Hedrick, R. M. Waymouth, *ACS Macro Lett.* **2012**, *1*, 845–847.
- 50 I. van der Meulen, Y. Y. Li, R. Deumens, E. A. J. Joosten, C. E. Koning, A. Heise, *Biomacromolecules* **2011**, *12*, 837–843.
- 51 H. Seyednejad, A. H. Ghassemi, C. F. van Nostrum, T. Vermonden, W. E. Hennink, *J. Control Release* **2011**, *152*, 168–176.
- 52 D. J. A. Cameron, M. P. Shaver, *Chem. Soc. Rev.* **2011**, *40*, 1761–1776.
- 53 A. E. van der Ende, J. Harrell, V. Sathiyakumar, M. Meschievitz, J. Katz, K. Adcock, E. Harth, *Macromolecules* **2010**, *43*, 5665–5671.
- 54 Y. Nagao, A. Takasu, *J. Polym. Sci., Part A: Polym. Chem.* **2010**, *48*, 4207–4218.
- 55 C. Jerome, P. Lecomte, *Adv. Drug Deliv. Rev.* **2008**, *60*, 1056–1076.
- 56 C. K. Williams, *Chem. Soc. Rev.* **2007**, *36*, 1573–1580.
- 57 J. E. Hudak, R. M. Barfield, G. W. de Hart, P. Grob, E. Nogales, C. R. Bertozzi, D. Rabuka, *Angew. Chem. Int. Ed.* **2012**, *51*, 4161–4165.
- 58 K. L. Christman, R. M. Broyer, E. Schopf, C. M. Kolodziej, Y. Chen, H. D. Maynard, *Langmuir* **2011**, *27*, 1415–1418.
- 59 J. M. Stukel, R. C. Li, H. D. Maynard, M. R. Caplan, *Biomacromolecules* **2010**, *11*, 160–167.
- 60 R. K. Iha, B. A. Van Horn, K. L. Wooley, *J. Polym. Sci., Part A: Polym. Chem.* **2010**, *48*, 3553–3563.
- 61 B. A. Van Horn, R. K. Iha, K. L. Wooley, *Macromolecules* **2008**, *41*, 1618–1626.
- 62 D. G. Barrett, M. N. Yousaf, *Macromolecules* **2008**, *41*, 6347–6352.
- 63 D. G. Barrett, B. M. Lamb, M. N. Yousaf, *Langmuir* **2008**, *24*, 9861–9867.
- 64 B. A. Van Horn, K. L. Wooley, *Soft Matter* **2007**, *8*, 1032–1040.
- 65 N. Spinelli, O. Prakash Edupuganti, E. Defrancq, P. Dumy, *Org. Lett.* **2007**, *9*, 219–222.
- 66 N. Dendane, A. Hoang, L. Guillard, E. Defrancq, F. Vinet, P. Dumy, *Bioconjugate Chem.* **2007**, *18*, 671–676.
- 67 K. L. Christman, R. M. Broyer, Z. P. Tolstyka, H. D. Maynard, *J. Mater. Chem.* **2007**, *17*, 2021–2027.
- 68 G. G. Kochendoerfer, J. M. Tack, S. Cressman, *Bioconjugate Chem.* **2002**, *13*, 474–480.
- 69 L. A. Marcaurette, Y. S. Shin, S. Goon, C. R. Bertozzi, *Org. Lett.* **2001**, *3*, 3691–3694.
- 70 L. A. Marcaurette, E. C. Rodriguez, C. R. Bertozzi, *Tetrahedron Lett.* **1998**, *39*, 8417–8420.
- 71 I. Taniguchi, W. A. Kuhlman, A. M. Mayes, L. G. Griffith, *Polym. Int.* **2006**, *55*, 1385–1397.
- 72 I. Taniguchi, A. M. Mayes, E. W. L. Chan, L. G. Griffith, *Macromolecules* **2005**, *38*, 216–219.
- 73 F. Lin, J. K. Zheng, J. Y. Yu, J. J. Zhou, M. L. Becker, *Biomacromolecules* **2013**, *14*, 2857–2865.

- 74** A. L. Silvers, C. C. Chang, T. Emrick, *J. Polym. Sci. Part A: Polym. Chem.* **2012**, *50*, 3517–3529.
- 75** Y. Yu, J. Zou, C. Cheng, *Polym. Chem.* **2014**, *5*, 5854–5872.
- 76** D. Tian, O. Halleux, P. Dubois, R. Jérôme, R. Sobryj, G. Van der Bossche, *Macromolecules* **1998**, *31*, 924–927.
- 77** D. Tian, P. Dubois, R. Jérôme, *Macromolecules* **1997**, *30*, 1947–1954.
- 78** D. Tian, P. Dubois, R. Jérôme, *Macromolecules* **1997**, *30*, 2575–2581.
- 79** D. Tian, P. Dubois, C. Grandfils, R. Jérôme, *Macromolecules* **1997**, *30*, 406–409.
- 80** D. Tian, P. Dubois, R. Jerome, *Macromol. Symp.* **1998**, *130*, 217–227.
- 81** J.-P. Latere Dwan'lsa, P. Lecomte, P. Dubois, R. Jérôme, *Macromol. Chem. Phys.* **2003**, *204*, 1191–1201.
- 82** J.-P. Latere, P. Lecomte, P. Dubois, R. Jérôme, *Macromolecules* **2002**, *35*, 7857–7859.
- 83** O. Persenaire, M. Alexandre, P. Degee, P. Dubois, *Biomacromolecules* **2001**, *2*, 288–294.
- 84** Y. Y. Yang, S. M. Dorsey, M. L. Becker, S. Lin-Gibson, G. E. Schumacher, G. A. Flaim, J. C. Kohn, C. G. Simon, *Biomaterials* **2008**, *29*, 1901–1911.
- 85** T. R. Olsen, L. L. Davis, S. E. Nicolau, C. C. Duncan, D. C. Whitehead, B. A. Van Horn, F. Alexis, *Acta Biomaterialia* **2015**, *20*, 94–103.